TERRA MOTAE

The Erzincan earthquake of 13 March 1992 in Eastern Turkey: tectonic aspects

Vladimir G. Trifonov[1], M. Salih Bayractutan[2], Arkadiy S. Karakhanian[3] and Tamara P. Ivanova[4]

[1]Geological Institute of the Russian Academy of Sciences, 7 Pyzhevsky, Moscow, 109017 Russia; [2]Earthquake Research Center of Ataturk University, 25240 Erzurum, Turkey; [3]Institute of Geological Sciences of the Armenian Academy of Sciences, 24a Marshal Bagramian Ave., Yerevan 37019, Armenia; [4]Institute of Mechanics of the Geosphere, Russian Academy of Sciences, Moscow 109017, Russia

SUMMARY

The tectonic significance of the Erzincan earthquake of 13 March, 1992 in Eastern Turkey is discussed. The intersection of the North Anatolian and The East Anatolian strike-slip fault zones has resulted in formation of the Erzincan pull-apart basin and new seismically active fault branches on its northeastern side. Local concentrations of surface ruptures strike along the most active branches of the North Anatolian fault zone (N300°W) for 62 km. They are usually open fractures with northeastern sides uplifted up to 20 cm and rarely with dextral offset up to 10 cm. These secondary ruptures manifest indirectly oblique seismic fault displacement corresponding to the Late Quaternary motion on the fault zone, although at the surface the dextral component has been suppressed relative to the vertical one.

Terra Nova, **5**, 184–189, 1993

INTRODUCTION

The $M = 6.8$ Erzincan earthquake occurred on 13 March 1992 with an epicentre close to the town of Erzincan and a focus probably in the upper crust. The earthquake caused significant damage in Erzincan and adjacent villages (Fig. 1) and caused 510 fatalities. A discontinuous N300°W-trending belt of small ruptures and landslides, 62 km long, was produced at the surface. The tectonic location of the earthquake, and the significance of its seismic ruptures are discussed in this paper.

TECTONIC POSITION

The Erzincan earthquake of 1992 occurred in the eastern part of the North Anatolian fault zone (NAFZ) (Fig. 2). The zone coincides here with the suture of the Meso-Tethys, closed in the middle and the late Cretaceous (Sengor *et al.*, 1980; Sengor and Yilmaz, 1981). A large ultrabasic massif is exposed in the Erzincan segment of the NAFZ. In the Eocene the Meso-Tethys suture was offset dextrally 300 km along a NW-trending fault, later inherited by the eastern part of the NAFZ (Bazhenov and Burtman, 1990). At the end of the Miocene or in the Pliocene dextral motion resumed and the fault zone extended to the west up to the Marmara Sea (Furon, 1953; Sengor and Yilmaz, 1981). Current dextral slip-rate close to Erzincan is estimated to be about 20 mm yr^{-1}.

Structurally the Erzincan region lies in a NW–SE-trending Pliocene–Quaternary

Fig. 1. *The aftermath of the 13 March 1992 Erzincan earthquake.*

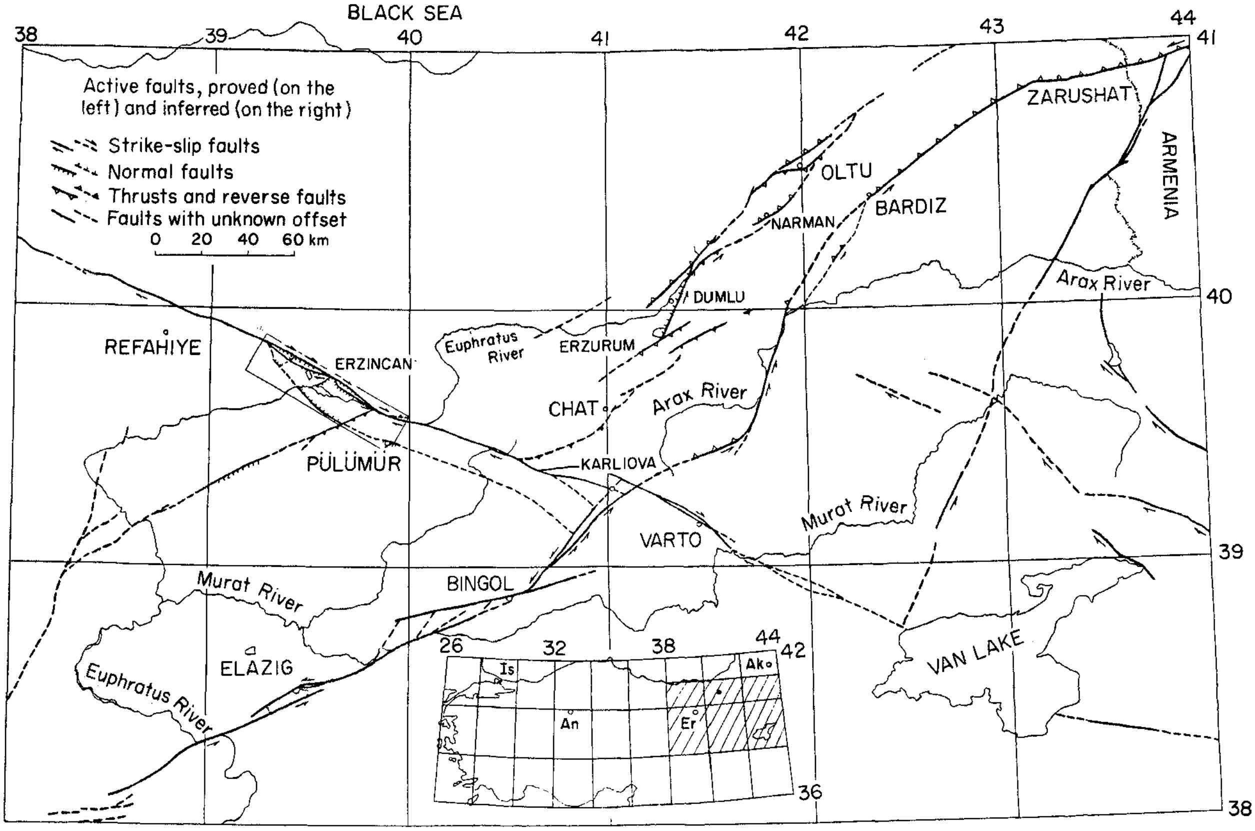

Fig. 2. *The faulting system in the Erzincan region (North Anatolian Fault Zone (NAFZ)).*

depression, occupied by the Euphrates valley in its southeastern part (Fig. 3). On both sides the depression is bounded by branches of the NAFZ. One of these faults is exposed near the road, 1 km to the south of the village of Eynyol, as a contact between the ultrabasites and the alluvial conglomerates of the Pliocene and Lower Quaternary. The fault plane is almost vertical (dips 80–90° to the SW) and strikes N300°W. The sandstone and gravel lenses in the conglomerates dip 50–70° to the south-west. The conglomerates are carbonatized near the contact.

The Late Pleistocene and Holocene activity of the fault zone is manifested along both sides of the basin by young scarps and facets. The latter are more spectacular on the northeastern side of the basin, delineating two (or three in some places) active fault branches with, as a rule, their northeastern sides uplifted (Fig. 3).

Three Middle or late Quaternary valleys are offset dextrally 1000 m along the 10 km long segment of the northeastern fault branch near the village of Yalnizbag Kö and to the north of Erzincan. To the north-east of Erzincan (near the village of Gechit Kö) the big ravine is offset 100 m and 15–20 m by northeastern and southwestern fault branches, respectively. The smaller streams are offset dextrally 8 m by the southwestern branch. Near the hills of the Altin-Tepe and Kara-Tepe (15–20 km to the south-east of Erzincan) the right-lateral offsets of the streams reach several tens of metres (up to 100 m).

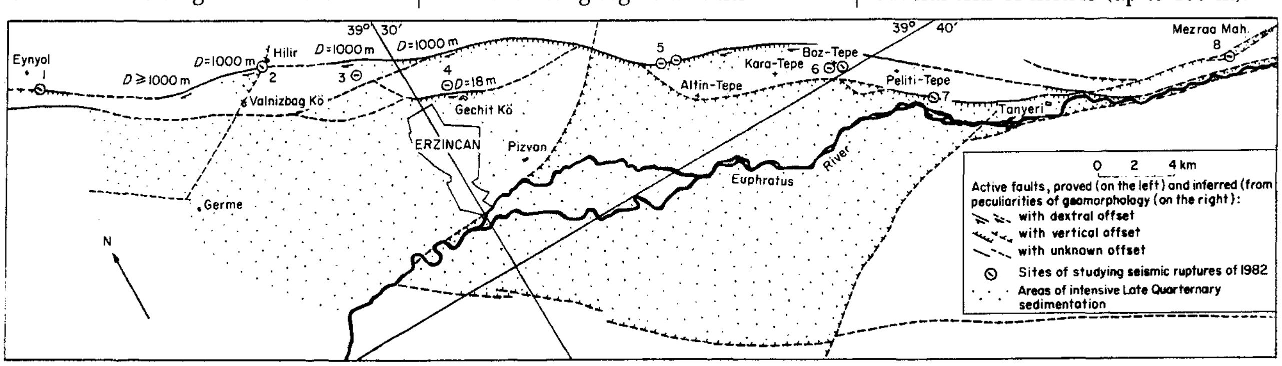

Fig. 3. *The boxed region around the town of Erzincan (see Fig. 2 for location in NAFZ).*

Tatar (1975) mapped similar offsets 50–60 km to the north-west of the Erzincan.

The active faults on both sides of the Erzincan basin merge to the north-west of Erzincan and continue to the south-east of the basins as separate branches. Immediately north of the village of Pülümür, faults continuing the southeastern fault branch form several scarps with their northeastern sides uplifted.

The NE-trending active faults although rarer, are also typical structural elements of the region. The largest Munzur fault bounds the Erzincan basin to the south-east, determining, together with NW-striking fault branches, its triangular form. The smaller ruptures differentiate areas of recent subsidence within the basin. For example, the fault between the villages of Hilir and Germe bounds an area of intensive sedimentation to the north-west and the fault near the village of Pizvan bounds the wider part of the Euphrates terrace to the north-west against a swampy plain. The minor NE-trending fault meets the continuation of the active faults on the southeastern side of the Erzincan basin close to the eastern edge of Pülümür. It was this fault that was reactivated by the strongest ($M = 5.8$) aftershock of the Erzincan earthquake on 18 March 1992. A N55–60°E-trending zone of open fractures and small scarps was created, along which the worst damage to construction was concentrated.

The generation of the Erzincan basin and coexistence of the NW- and the NE-trending Quaternary faults can be understood in terms of the interaction between the NAFZ and the East Anatolian fault zone (EAFZ) (Fig. 2). To the west of where the NAFZ and the main strand of the EAFZ intersect near Karliova (Fig. 2), the NAFZ is represented by at least three branches, the southern branch being the oldest and the northern branch being the youngest. Only the northern branch continues to the east of the crossing. The same geometry is found on the EAFZ to the south-west of the intersection, where only the youngest southeastern branch continues to the north-east of the crossing.

These geometrical peculiarities can be explained by the evolving tectonics of the fault junction (Fig. 4). Strike-slip movement along one fault continually offsets the other.

The NAFZ has attracted considerable scientific interest as a result of a series of strong 20th century earthquakes (Allen, 1975; Ambraseys, 1970, 1975, 1988; Pavoni, 1961; Wallace, 1968). Three quarters of the fault zone was reactivated from 1912 to 1976 with a total dextral offset of up to 4.5 m and a vertical displacement up to 2.5 m (5 m on two short segments). The largest earthquake ($M = 7.8$) took place on 26 December, 1939, near Erzincan, for which the seismic rupture zone extended for a distance of 350 km with a dextral offset up to 3.7 m and the vertical shift up to 2 m.

Seventeen earthquakes with $M >= 6$ have occurred along the NAFZ in the 20th century (before 1992), but only three or four similar shocks took place during each of the three previous centuries (Ambraseys, 1989). Recent work by A. S. Karakhanian and A. O. Asatrian employing previously unresearched Armenian manuscripts indicates an earlier active epoch prior to the 16th century commensurable with that of the 20th century. So, at least two seismic episodes have taken place here, the intervening seismic cycle lasting approximately 500 years. The Erzincan region stands out even with respect to the high seismicity of other parts of the NAFZ. Forty-six earthquakes with intensity $I >= 8$ and possible magnitude $M >= 5.5$ are known to have occurred here since AD 802.

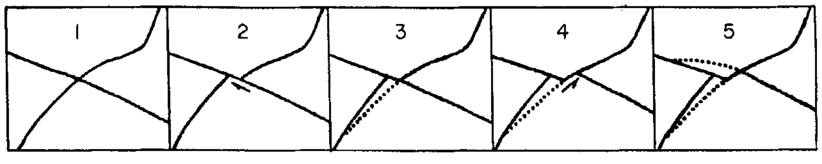

Fig. 4. *The progressive development of the fault junction tectonics.*

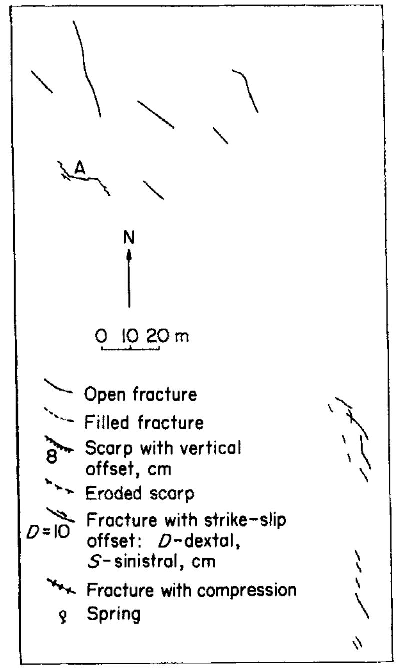

Fig. 5. En echelon *short fractures at the northwestern end of the Erzincan seismic rupture belt near the village of Hilir.*

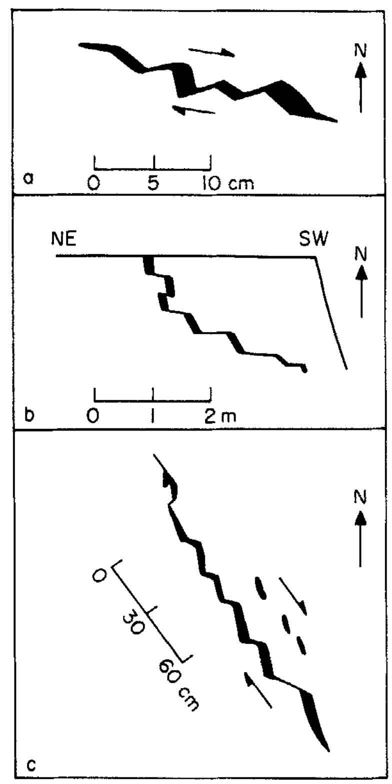

Fig. 6. *Diagrammatical representation of the features shown in Fig. 7.*

(a) (c)

Fig. 7. *(a) Rupture 'A' on Fig. 5; closed N80°E-trending segment; (b) broken southern wall of the Eshkesu reservoir on Fig. 9; (c) NW-trending scarp on the northeastern bank of the Euphrates River (D on Fig. 10).*

(b)

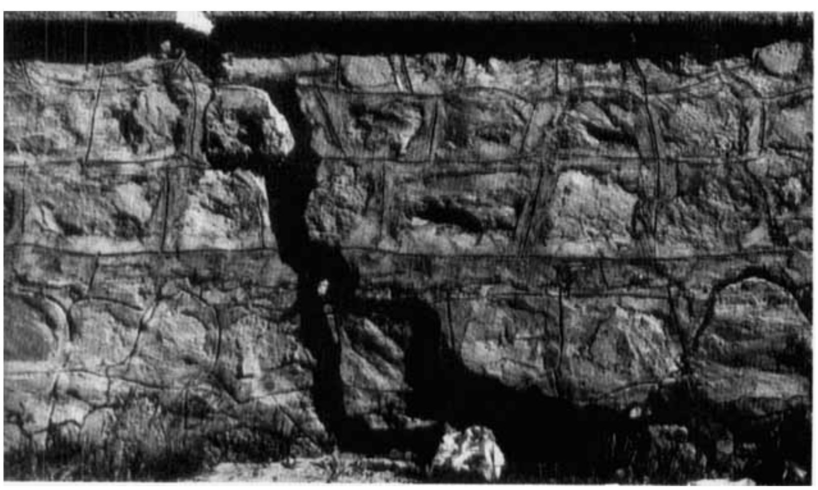

THE 1992 SEISMIC RUPTURES

Seismic ruptures connected with the March 13, 1992 earthquake are found in a 62 km long belt along the northeastern side of the Erzincan basin (Fig. 3), striking N290–300°W. The fractures are usually open, and irregular, sometimes with uplifted northeastern sides. Several characteristic clusters of fractures are described below passing NW–SE of the belt.

1 Several N300°W-trending open fractures break the road cover 1 km to the south of the village of Eynyol, following the contact between ultrabasites and conglomerates, mentioned above. One N330°W-trending open crack breaks the artificial soil near the road along strike to the north-west.

2 The surface of the alluvium fan covering the northeastern branch of the NAFZ 0.5 km to the south-east of the village of Hilir is broken by fractures striking predominantly N325°W ± 10°. They form a N325°W-trending band, 240 m long. Short (up to 10 m) fractures at the southeastern end of the band are arranged *en echelon* to each other and form a N-trending row (Fig. 5). The rupture (A) has a zigzag pattern, the central section striking W280°N; its short N310–340°W-trending segments are open while the N80°E-trending segments are closed (Figs 6a, 7a). As a whole these patterns are manifestations of the dextral kinematics of the rupture.

One hundred metres to the north-west of the band a short, open N20°E-trending fracture is observed. A 12 m-long NW-trending scarp with uplifted northeastern side is seen 150 m further on. Along the latter small water springs smelling of sulfur and burnt grass were found.

3 NW-trending open fractures break the road cover 3.5 km to the north of Erzincan, between two active branches of the NAFZ.

4 Near the village of Gechit Kö, 1 km to the NE of Erzincan, ruptures break the southern slope and the top of the hill near the southeastern active fault branch of the NAFZ. They form a N290°W-trending *en echelon* row, 210 m long (Fig. 8), with individual ruptures striking N300–340°W. They are dilated up to 3 cm, their northeastern sides uplifted by up to 10 cm. Along two fractures 1.5 cm of left lateral slip and 2.5 cm of right-lateral slip have been measured, respectively. Since ruptures continue to the flat top of the hill and the westernmost one breaks both slopes of an adjacent ravine with the same sense of offset, the vertical throw appears to have some tectonic origin.

5 Ruptures breaking artificial and (in the eastern part) natural soils surface between the Eshkesu mineral spring and several mineral springs in the swamp to the east of Eshkesu. They form a W280°N-trending wide, 240 m long band (Fig. 9), in which most of the *en echelon* ruptures strike N280–350°W. Most of the ruptures are open and the northern, eastern or northeastern sides

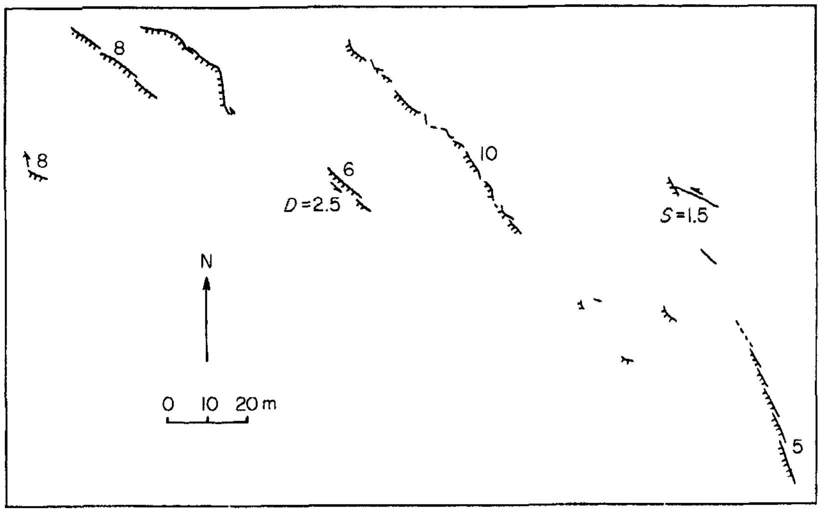

Fig. 8. En-echelon *row of ruptures near the village of Gechit Kö.*

are uplifted up to 20 cm. The ruptures break the concrete sides of a reservoir at the northwestern end of the band, with concrete blocks thrust up to 4 cm. On the 2 m-high southern wall of the reservoir one superficial fracture widens upwards from 6 cm to 15 cm (Figs 6b and 7b).

Two almost parallel NW-trending fractures break the narrow irrigational channel 0.8 km to the south-east of the Eshkesu spring, with a dextral offset of 3 cm on the northeastern fracture and a sinistral offset of 2 cm on the southwestern fracture.

6 The southwestern slope of the Boz–Tepe Pliocene–Quaternary volcano is broken by an open fracture with its northeastern side uplifted 5 cm accompanied by smaller fractures, all of them striking N310°W with local deviations to W290°N. The edge of the alluvium terrace is broken, 0.4 km to the SE of the top of the hill, by several short fractures, striking N350°W, that form a N-trending *en echelon* row.

7 Two concentrations of ruptures have been discovered on the surface of the lowest saturated and swampy terrace on the northeastern bank of the Euphrates River, 6–7 km to the NW of the Tanyeri railway station, between the highway and the railway, that was deformed during the earthquake.

The eastern concentration is a NW-trending band of open fractures and scarps with northeastern sides uplifted up to 12 cm (Figs 10, right, and 7c). One of the ruptures (Fig. 6c) is represented by a zigzag combination of the N350–0°W-trending open segments and the W270–290 N-trending closed segments. Calculations show that the amount of dextral slip could be about 10–12 cm. The band continues onto the highway cover.

The western concentration is situated 200 m away and comprises a semicircular system of fractures with uplifted northern and eastern sides (Fig. 10, left). Some fractures are traced by patches of burnt grass. Here as well as at site 2, the grass had burnt out before the final melting of the snow, i.e. apparently during the earthquake. The same phenomena took place during the Spitak earthquake of December 7, 1988 (Trifonov *et al.*, 1990). In both cases this could be accounted for by ignition of discharging methane.

8 The concrete bridge on the road 2.5 km to the WSW of the village of Mezraa Mah is broken by a NW-trending fracture with 16 cm of sinistral offset (Fig. 11). A dextral offset of 6 cm takes place on a smaller N-trending fracture. An *en echelon* row of NNW-trending open fractures breaks the lower terrace to the SE of the bridge.

Thus the seismic ruptures created on the land surface during the earthquake, are characterized by the following peculiarities:

(i) All ruptures (except Boz-Tepe fractures) break Quaternary unconsolidated sediments. The biggest concentrations of fractures are found in artificial soils or saturated alluvium, often bordering water.

(ii) Fracture openings typically of 2–3 cm, rarely up to 10 cm, are found. The magnitude of opening decreases rapidly downwards (as is seen near the Eshkesu spring). The same decay of opening was observed along seismic ruptures of the Kum Dagh, 1983, and the Spitak 1988, earthquakes (Trifonov *et al.*, 1986, 1990), and shows that the cracks are superficial, caused by changes in soil properties near the surface.

(iii) A vertical throw of up to 20 cm is represented by scarps commonly with their northeastern sides uplifted. This sense of the uplift is characteristic for all slopes, not only those dipping south-east, thus revealing the general tendency of Quaternary vertical throws along faults on the northeastern side of the Erzinican basin.

(iv) Individual ruptures are often arranged *en echelon*. The ruptures strike N300–350°W, obliquely to the general trend (N290–300°W) of the rupture belt. Some individual ruptures comprise N-

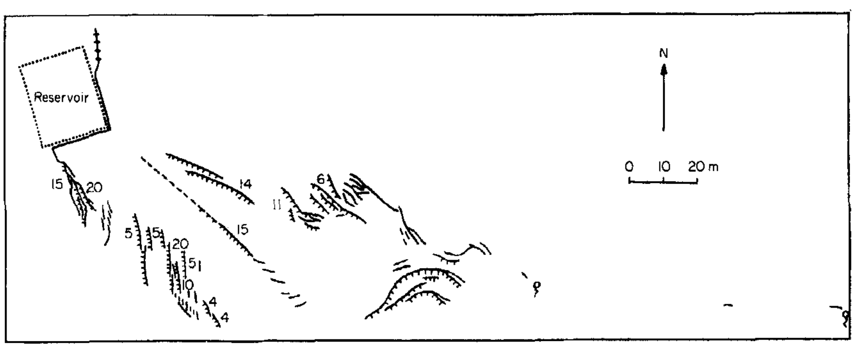

Fig. 9. En-echelon *band of ruptures near Eshkesu; most ruptures strike N280–350° W.*

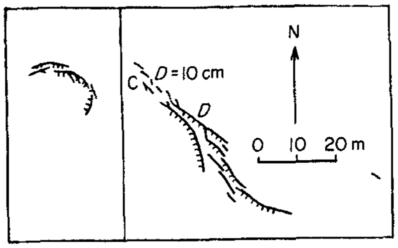

Fig. 10. *The western concentration of ruptures with uplifted northern and eastern sides on the bank of the Euphrates River (left); eastern concentration of ruptures in the same area. C is shown in Fig. 6c and D is shown in Fig. 7c.*

or NW-striking open, and WNW- or the W-striking closed, segments. All these manifest dextral displacement along the rupture belt, though the observed right-lateral offsets are not more than 12 cm. Left-lateral offsets observed across several fractures do not exceed 1.5 cm. 16 cm of apparent left-lateral shift measured on a concrete bridge near Mezraa Mah seems to reflect peculiarities of bridge failure.
(v) The rupture belt follows the Erzinican basin segment of the NAFZ. Single ruptures and their concentrations are situated on active fault branches of the NAFZ or in between them.

DISCUSSION

A number of features of the seismic ruptures of 13 March 1992 testify to their secondary origin, resulting from ground motion affecting near-surface strata. These include the concentration in loose sediments, their higher density in the artificial soils and saturated deposits. At the same time the overall configuration of ruptures relative to the active fault zone and the similarities between the kinematics and relations of ruptures (dextral slip with uplift of the northeastern sides) and the Quaternary faulting suggests that they indirectly reflect oblique displacement along the fault with a predominance for displaying the vertical component of slip. The same predominance of vertical throw over lateral displacement on the faults of the NAFZ manifested itself during the $M = 7.3$ Ilgax-Ladik earthquake of 26 November 1943 (Ambraseys, 1975, 1988).

ACKNOWLEDGEMENTS

Our 1991–92 research work could not have been undertaken without the support of the International Lithosphere Program, its President Professor A. M. Bally and the Secretary-General M. J. Berry, as well as of the Ataturk University in the Erzurum, Turkey, and especially its Rector Professor H. Ertugrul. The Governor of the Erzincan Vilayet and his administration helped us to carry out field studies under difficult conditions after the earthquake. Dr E. Vittori (ENEA-DISP, Rome, Italy), and Eng. A. Chatzipetros (the Aristole University, Thessaloniki, Greece) participated in these works. The authors thank all of them very much.

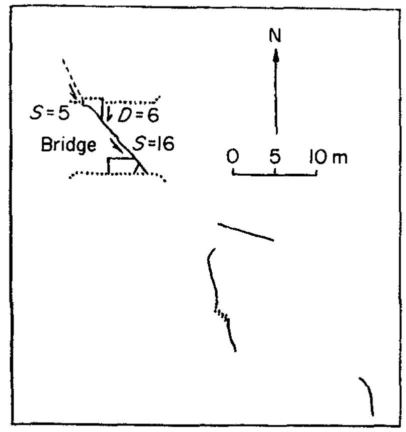

Fig. 11. *Broken concrete bridge near the village of Mezraa Mah.*

REFERENCES

Allen C.R. (1975) Geological criteria for evaluating seismicity, *Bull. geol. Soc. Am.*, **86,** 1041–1057.

Ambraseys N.N. (1970) Some characteristic features of the North Anatolian fault zone, *Tectonophys.*, **9,** 143–165.

Ambraseys N.N. (1975) Studies in historical seismicity and tectonics, *Geodynamics Today*, Royal Society Press, London, 7–16.

Ambraseys N.N. (1988) Engineering seismology, Earthquake engineering and structural dynamics, 17, 1–105.

Bazhenov M.L. and Burtman V.S. (1990) *Structural Arcs of the Alpine Belt: Carpathians–Caucasus–Pamirs*. Nauka Press, Moscow, 167 pp. (in Russian).

Furon R. (1953) Introduction à la géologie et a la hydrogéologie de la Turquie, *Mem. Mus. Natl. Hist. nat. Paris*, **3,** 144 pp.

Pavoni N. (1961) Die nordanatolische Horrizontalschiebung, *Geol. Rdsch.*, **51,** 122-139.

Sengor A.M.S., Yilmaz Y. and Ketin J. (1980) Remnants of a pre-Late Jurassic ocean in Northern Turkey: Fragments of Permian–Triassic Paleo-Tethys?, *Bull. geol. Soc. Am.*, **91,** 591–609.

Sengor A.M.S. and Yilmaz Y. (1981) Tethyan evolution of Turkey: A plate tectonic approach, *Tectonophys.*, **75,** 181–241.

Tatar Yu. (1975) Tectonic structures along the North Anatolian fault zone, northeast of Refahiye (Erzincan), *Tectonophys.*, **29,** 401–409.

Trifonov V.G., Lykov V.I., Vostrikov G.A., Orazsahatov H. and Scobelev S.F. (1986) Tectonic aspects of the Kum Dagh earthquake of 1983 in western Turkmenia, *Izvestiya (News) USSR Acad. Sci., Geol. Ser.*, **5,** 3–16 (in Russian).

Trifonov V.G., Karakhanian A.S. and Kozhurin A.I. (1990) The Spitak earthquake as a manifestation of recent tectonic activity, *Geotectonics*, **24,** 517–530.

Wallace R.E. (1968) Earthquake of August 19, 1966. Varto area, Eastern Turkey, *Bull. seism. Soc.*, **58,** 11-45.